Atomtronic Circuits of Diodes and Transistors

R. A. Pepino, J. Cooper, D. Z. Anderson, and M. J. Holland

JILA, National Institute of Standards and Technology and Department of Physics, University of Colorado,
Boulder, Colorado 80309, USA

We illustrate that open quantum systems composed of neutral, ultracold atoms in one-dimensional optical lattices can exhibit behavior analogous to semiconductor electronic circuits. A correspondence is demonstrated for bosonic atoms, and the experimental requirements to realize these devices are established. The analysis follows from a derivation of a quantum master equation for this general class of open quantum systems.

Atomtronics [1] focuses on ultracold atom analogs of electronic circuits and devices. Previous work has established the possibility of diode [2,3] and transistor [4–6] behavior in atomic systems. We calculate the device characteristics of these semiconductorlike systems by construction of complete atomtronic circuits. Such circuits contain the analog of electronic power supplies or batteries and the necessary device connections. This opens up the possibility for more complex circuits in which atomtronic device components can be cascaded. The approach that we introduce develops a general theoretical method for solving the dynamics of strongly interacting, many-body, *open* quantum systems.

A diode is in essence a device which exhibits an asymmetric response; applying a potential gradient one way leads to a large current and the opposite way leads to virtually no current. The atomtronic diode that we present is novel compared to some previously proposed devices [2,3] in that it does this without relying on an intrinsic irreversibility of the device itself (e.g., the spontaneous emission of a photon or phonon). The atomtronic transistor presented here contrasts with other proposals [4,5], in that it operates in the steady state rather than only in an initial (transient) regime. It also reproduces the essential transistor behavior, including the control of a larger atomtronic current with a smaller one, and the ability to perform digital logic and exhibits linear amplification. One motivation for designing atomtronic diode and transistor components that are intrinsically reversible is that they can then be combined in quantum computing applications where coherent logic is required.

This topic is relevant for the emerging field of strongly correlated dynamical and nonequilibrium phenomena in ultracold atomic gases [7–10]. Atomtronic devices require site-by-site control of the temporal or spatial properties of optical lattices [11–14], a common goal for numerous experiments aiming to utilize optical lattices for quantum control, quantum transport, quantum computing, and quantum simulation [15–17]. What is novel here is that the atomtronic systems that we consider are open quantum systems, meaning that they are composed of optical lattices coupled to two or three reservoirs, with the reservoirs acting as sources or sinks for particles.

The Hamiltonian takes the separable form

$$\hat{H} = \hat{H}_{\text{sys}} + \hat{H}_{\text{res}} + \hat{H}_V, \tag{1}$$

where $\hat{H}_{\text{sys}}$ and $\hat{H}_{\text{res}}$ denote system and reservoir Hamiltonians, respectively, and $\hat{H}_V$ their interaction. Although atomtronic devices can utilize either fermionic or bosonic atoms, we focus our discussion on the bosonic case, providing contrast with electronics where the carriers are fermionic. In the lowest band approximation, $\hat{H}_{\text{sys}}$ is the Bose-Hubbard Hamiltonian that describes ultracold bosons in a one-dimensional optical lattice [12,18,19], given by

$$\hat{H}_{\text{sys}} = -\sum_{\langle i,j \rangle} J_{ij}\hat{a}_i^\dagger \hat{a}_j + \sum_i \left(\epsilon_i \hat{N}_i + \frac{U}{2}\hat{N}_i(\hat{N}_i - 1) \right), \tag{2}$$

where site i has energy ϵ_i, interaction energy U, and annihilation and number operators $\hat{a}_i$ and $\hat{N}_i = \hat{a}_i^\dagger \hat{a}_i$, respectively, and J_{ij} is the hopping energy between adjacent sites i and j. To achieve a steady-state current, atomtronic circuits require two or more reservoirs held at different chemical potentials. The free Hamiltonian for the reservoirs is

$$\hat{H}_{\text{res}} = \sum_{\nu,l} \hbar \omega_{\nu l} \hat{R}_{\nu l}^\dagger \hat{R}_{\nu l}, \tag{3}$$

where ν identifies the mode of reservoir l with energy $\hbar \omega_{\nu l}$ and annihilation operator $\hat{R}_{\nu l}$. It is assumed that each reservoir is so large that its thermodynamic properties are parametrized by a constant chemical potential μ_l and temperature T_l. Each reservoir is connected to a single system site s_l so that the interaction between the system and reservoir can be written as

$$\hat{H}_V = \sum_{\nu,l} g_{\nu l} \hat{R}_{\nu l}^\dagger \hat{a}_{s_l} + \text{H.c.}, \tag{4}$$

where $g_{\nu l}$ are the system-reservoir hopping energies.

Our atomtronic analog of electronic circuits begins with the definition of the atomtronic battery, composed of two reservoirs of ultracold atoms having different chemical potentials, corresponding to different electric potentials at the terminals of a conventional battery. In Fig. 1(a), we show an electronic circuit composed of a diode connected to a battery by resistive wires. In Fig. 1(b), the atomtronic equivalent of this diode is the part of the lattice that is enclosed by a dashed box with the lattice site energy on the left half offset from the lattice site energy on the right half. To the left and right of the diode are the reservoirs at high and low chemical potentials, respectively. These are the analogs of the battery terminals. The system-reservoir separation is provided by large tunneling barriers that ensure weak coupling. The explicit physical implementation for the reservoirs shown is an optical lattice in the zero-temperature Mott-insulator phase. In this system, strong interactions lead to a fermionization of the bosons giving a broad continuum of reservoir modes fully occupied below the chemical potential.

In the situation described, we find that the current response depends strongly on the direction of the applied chemical potential difference. The atomtronic diode's conduction asymmetry becomes optimal when the height of the potential step in the middle of the diode is equal to the on-site interaction energy U. This general behavior is observed not only for the six-site lattice shown but also for lattices containing variable numbers of sites. In order to explain the general mechanism, we consider the simplest case of a two-well system with potential offset U and connected on each side to a reservoir. An appropriate basis for this two-site case is the number basis $|n, m\rangle$, where n and m are the numbers of atoms in the left and right wells, respectively.

As shown pictorially in Fig. 2, the potential offset sets up a degeneracy between two states. The state $|2, 0\rangle$ is resonantly coupled to the state $|1, 1\rangle$ (double-headed arrow), and both remain separated in energy from $|0, 2\rangle$. The reverse-bias situation is shown in Fig. 2(a). If the chemical potentials for both the left reservoir μ_L and right reservoir μ_R are initially sufficiently low, the system begins in an equilibrium devoid of particles. Raising μ_R from this point leads to populating the $|0, 1\rangle$ state. Since this state is detuned from $|1, 0\rangle$ by the on-site interaction energy U, the steady-state dynamics corresponds to virtually no current flow. Further raising of μ_R allows the state $|0, 2\rangle$ to be occupied. This state is detuned from $|1, 1\rangle$ by $2U$. As a result, there is again no effective transport across the lattice system.

However, if μ_R is reset to its initial low value and μ_L raised, the resulting forward-bias dynamics are quite different. As shown in Fig. 2(b), when μ_L is increased to the point where the $|2, 0\rangle$ state is occupied, this opens up the possibility for resonant transport of atoms from the left reservoir to the right reservoir via the two resonant current loops: $|2, 0\rangle \to |1, 1\rangle \to |1, 0\rangle \to |2, 0\rangle$ and $|2, 0\rangle \to |1, 1\rangle \to |2, 1\rangle \to |2, 0\rangle$.

This qualitative picture of the diode operation is supported in detail by the solution of the quantum dynamics for the open quantum system. We solve for the evolution of the reduced density operator of the system $\hat{\sigma} \equiv \mathrm{Tr}_{\mathrm{res}}[\hat{\rho}]$, in which $\hat{\rho}$ is the full density operator of the system and reservoir and the trace is over the reservoir degrees of freedom. Under the Born-Markov approximation, the evolution of $\hat{\sigma}$ is given by the master equation [20–22]

$$\left(\frac{d}{dt} + i\hat{\mathcal{L}}_{\mathrm{sys}}\right)\hat{\sigma}(t) = \int_0^\infty d\tau \hat{R}(\tau)\hat{\sigma}(t), \qquad (5)$$
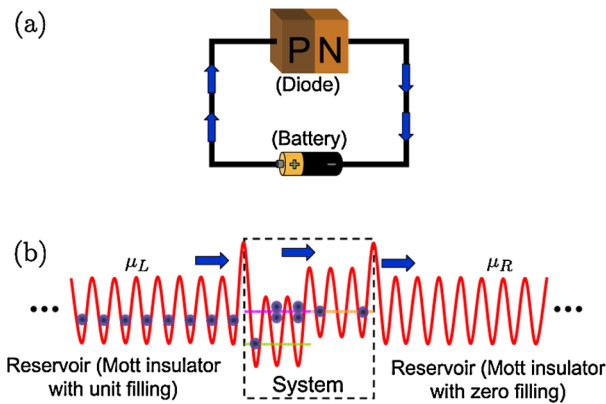
(a)

(b)

FIG. 1 (color online). (a) An electronic circuit with a battery, resistive wires, and a p-n junction diode in the forward bias and (b) the atomtronic equivalent. The left reservoir has chemical potential μ_L and unit filling and supplies atoms that flow through the system (dashed box) to the right reservoir, with chemical potential μ_R and zero filling. The weak system-reservoir coupling is ensured by large tunneling barriers at each interface.
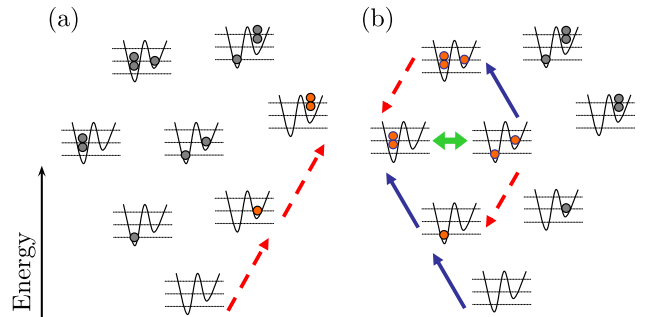
(a)   (b)

FIG. 2 (color online). Dynamical path of an initially empty two-well lattice system. The vertical axis corresponds to the energy of the system's quantum states. The solid (blue) and dashed (red) arrows indicate the transfer of atoms from the left and right reservoirs, respectively. (a) Reverse bias (low left-hand chemical potential and high right-hand chemical potential). Here the system evolves into the $|0, 2\rangle$ dark state where it becomes trapped. (b) Forward bias (high left-hand chemical potential and low right-hand chemical potential). The resonance between $|2, 0\rangle$ and $|1, 1\rangle$, shown by the double-headed (green) arrow, allows the resonant transport of atoms across the lattice.

where the memory kernel is

$$\hat{R}(\tau) = \text{Tr}_{\text{res}}\{i\hat{\mathcal{L}}_V \exp[-i\tau(\hat{\mathcal{L}}_{\text{sys}} + \hat{\mathcal{L}}_{\text{res}})]i\hat{\mathcal{L}}_V\}. \quad (6)$$

Here the Liouville operators $\hat{\mathcal{L}}_{\text{sys}}$, $\hat{\mathcal{L}}_{\text{res}}$, and $\hat{\mathcal{L}}_V$ are defined

via commutators of their respective Hamiltonians; i.e., for operator $\hat{\Theta}$, $\hbar\hat{\mathcal{L}}_X\hat{\Theta} = [\hat{H}_X, \hat{\Theta}]$, $X \in \{\text{sys, res, } V\}$.

Substituting Eq. (6) into Eq. (5) yields the following closed form that is sufficiently simple to solve numerically:

$$\frac{d\hat{\sigma}}{dt} - \frac{1}{i\hbar}[\hat{H}_{\text{sys}}, \hat{\sigma}] = -\frac{1}{\hbar^2}\sum_l |g_l|^2 \sum_\nu \int_0^\infty d\tau e^{-\eta\tau}\{[\hat{a}_{s_l}, \hat{a}_{s_l}^\dagger(-\tau)\hat{\sigma}]\langle\hat{R}_{\nu l}^\dagger\hat{R}_{\nu l}(-\tau)\rangle - [\hat{a}_{s_l}, \hat{\sigma}\hat{a}_{s_l}^\dagger(-\tau)]\langle\hat{R}_{\nu l}(-\tau)\hat{R}_{\nu l}^\dagger\rangle$$
$$+ [\hat{a}_{s_l}^\dagger, \hat{a}_{s_l}(-\tau)\hat{\sigma}]\langle\hat{R}_{\nu l}\hat{R}_{\nu l}^\dagger(-\tau)\rangle - [\hat{a}_{s_l}^\dagger, \hat{\sigma}\hat{a}_{s_l}(-\tau)]\langle\hat{R}_{\nu l}^\dagger(-\tau)\hat{R}_{\nu l}\rangle\}, \quad (7)$$

with $\hat{a}_{s_l}(-\tau) = \exp(-i\hat{H}_{\text{sys}}\tau)\hat{a}_{s_l}\exp(i\hat{H}_{\text{sys}}\tau)$ and $\hat{R}_{\nu l}(-\tau) = \exp(-i\hat{H}_{\text{res}}\tau)\hat{R}_{\nu l}\exp(i\hat{H}_{\text{res}}\tau)$ defining the system and reservoir operators, respectively, in the interaction picture. The parameter η regularizes the integral and remedies the infrared divergence that is needed to account correctly for the beyond Born-Markov effects that arise from the coupling of near degenerate system-reservoir levels [23]. The theory should be cutoff and renormalized to account properly for the ultraviolet divergence that arises from the replacement in Eq. (7) of $g_{\nu l}$ by one that is mode independent, i.e., $g_{\nu l} = g_l$.

The numerical solution of the diode connected to a reservoir of this type in the steady state is shown in Fig. 3. The reverse bias (inset) shows virtually no current response as a function of the chemical potential difference, and the forward-bias case exhibits a turn-on of the current at the point where the resonance states previously discussed become occupied. As anticipated from the qualitative picture given earlier, when the current turns on, there are two observable steps associated with linear combinations of the two possible resonant current loops, with a rise broadened by η.

Building on this understanding of the diode, we now develop the atomtronic transistor. Since a transistor is a three-terminal device, transistor action requires at least three lattice sites connected to three independent reser-

voirs. As seen in Fig. 4, the middle well is shifted down in energy by U with respect to both the left and right wells. To investigate the device characteristics, we put a fixed bias across the transistor. This means that μ_L is higher than the value necessary to give an occupancy of one atom on the left system site, and μ_R is below the value needed to deplete all atoms on the right system site. We then study the system's steady-state response to an increase of the middle chemical potential μ_M.

When μ_M is low, the middle site contains virtually no atoms, and the system is locked in $|1, 0, 0\rangle$. This state is only weakly coupled to $|0, 0, 1\rangle$ via a second-order off-resonant process through $|0, 1, 0\rangle$. As the middle chemical potential is raised, a nonzero occupancy results on the middle site, and a resonance is accessed among the states $|1, 1, 0\rangle$, $|0, 2, 0\rangle$, and $|0, 1, 1\rangle$. This triggers a cycle that corresponds to a significant current across the system, as shown in Fig. 4. High linear differential gain (inset) is achieved by ensuring that the system-reservoir coupling g_l in Eq. (7) is smaller in magnitude for the middle reservoir compared to the left and right couplings. The
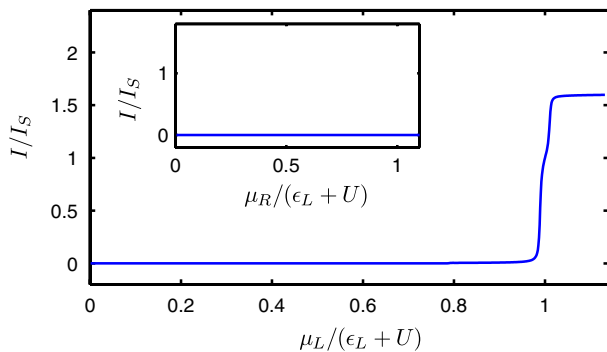

FIG. 3 (color online). Current of the forward-bias and reverse-bias (inset) response for the diode. The horizontal axes are the chemical potential difference normalized to the resonance value. The vertical axes are the resulting current responses normalized to the saturation current I_S that arises when the normalized chemical potential difference is unity.
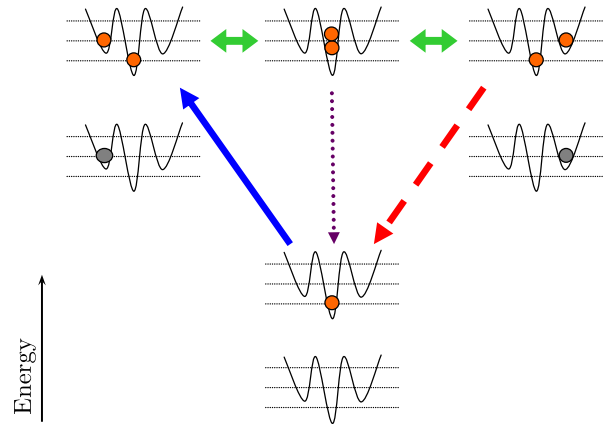

FIG. 4 (color online). The level scheme for the atomtronic transistor with a fixed chemical potential difference across the system. The base potential is set to put one particle on the middle site, which triggers a resonance that allows for transport across the system. The left, right, and middle reservoir dynamics are represented by solid (blue), dashed (red), and dotted (purple) arrows, respectively, while intrasystem dynamics are represented by double-headed (green) arrows.
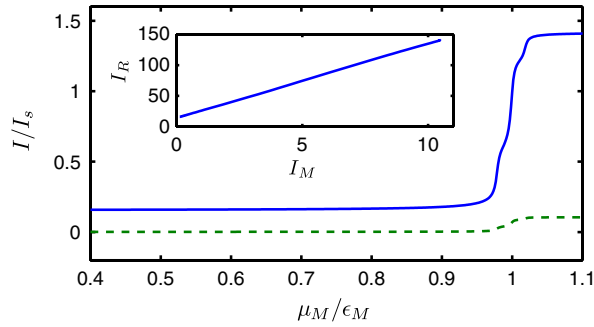
FIG. 5 (color online).   The current response and differential gain of the atomtronic transistor are plotted. In this simulation, the reservoir couplings g_l for the left and right reservoirs are 5 times that of the middle reservoir. For fixed $\mu_L - \mu_R$, we vary μ_M and record the response of currents leaving the system from the right site (blue solid curve) and from the middle site (green dashed curve). Here I_S is the current value of the emitter when $\mu_M = \epsilon_M$. The inset is a plot of the right current versus the middle current, from which a large linear differential gain is apparent.

current that results from the $|0, 2, 0\rangle$ to $|0, 1, 0\rangle$ transition, i.e., an atom leaving the system and entering the middle reservoir, is then much smaller than the current which flows from left to right across the device. In Fig. 5, results are plotted of the numerical simulation for the case in which the middle reservoir coupling is one-fifth that of the reservoirs on either end.

In conclusion, we have calculated device characteristics of simple diode and transistor atomtronic circuits. We have focused here on the two-site and three-site models to simplify the presentation, but full calculations for more extended systems with a greater site number confirm that the diodelike and transistorlike behavior persists. This work motivates expansion of the analogy to more complex circuits, such as amplifiers, constant current sources, flip-flops, and logic elements. Apart from their potential practical value, it would be intriguing to consider the connection of atomtronics with quantum information physics and quantum computation, since computers are based on cascaded logic devices and these atom devices presented operate exclusively in the coherent regime.

Atomtronic devices will always be much slower than their electronic counterparts. For example, the overall current flow is determined principally by the tunneling rate from one site to the next [1]. Compensating for this is the fact that atomtronic studies are pursuing device physics in a novel physical system: Unlike electrons, atoms have a complex internal structure and internal states, the atoms can be bosons or fermions, they are massive and affected by gravitational and electromagnetic fields, the material itself which is the optical lattice can be dynamically and spatially varied, and many unavoidable effects present in solid-state systems such as crystalline impurities, dislocations, and phonon scattering are absent.

[1] B. T. Seaman, M. Krämer, D. Z. Anderson, and M. J. Holland, Phys. Rev. A **75**, 023615 (2007).
[2] A. Ruschhaupt and J. G. Muga, Phys. Rev. A **70**, 061604 (R) (2004).
[3] A. Ruschhaupt, J. G. Muga, and M. G. Raizen, J. Phys. B **39**, 3833 (2006).
[4] J. A. Stickney, D. Z. Anderson, and A. A. Zozulya, Phys. Rev. A **75**, 013608 (2007).
[5] A. Micheli, A. J. Daley, D. Jaksch, and P. Zoller, Phys. Rev. Lett. **93**, 140408 (2004).
[6] J. Y. Vaishnav, J. Ruseckas, C. W. Clark, and G. Juzelunas, Phys. Rev. Lett. **101**, 265302 (2008).
[7] D. Jaksch and P. Zoller, Ann. Phys. (N.Y.) **315**, 52 (2005).
[8] I. Bloch, J. Dalibard, and W. Zwerger, Rev. Mod. Phys. **80**, 885 (2008).
[9] I. Bloch, J. Phys. B **38**, S629 (2005).
[10] E. Altman, A. Polkovnikov, E. Demler, B. I. Halperin, and M. D. Lukin, Phys. Rev. Lett. **95**, 020402 (2005).
[11] O. Morsch and M. Oberthaler, Rev. Mod. Phys. **78**, 179 (2006).
[12] M. Greiner, O. Mandel, T. Esslinger, T. W. Hänsch, and I. Bloch, Nature (London) **415**, 39 (2002).
[13] T. Stöferle, H. Moritz, C. Schori, M. Köhl, and T. Esslinger, Phys. Rev. Lett. **92**, 130403 (2004).
[14] B. Paredes *et al.*, Nature (London) **429**, 277 (2004).
[15] I. Bloch, Nature (London) **453**, 1016 (2008).
[16] T. Calarco, U. Dorner, P. S. Julienne, C. J. Williams, and P. Zoller, Phys. Rev. A **70**, 012306 (2004).
[17] G. De Chiara *et al.*, Phys. Rev. A **77**, 052333 (2008).
[18] D. Jaksch, C. Bruder, J. I. Cirac, C. W. Gardiner, and P. Zoller, Phys. Rev. Lett. **81**, 3108 (1998).
[19] J. H. Denschlag *et al.*, J. Phys. B **35**, 3095 (2002).
[20] P. Meystre and M. Sargent III, *Elements of Quantum Optics* (Springer, New York, 1999).
[21] C. C. Tannoudji, J. D. Roc, and G. Grynberg, *Atom-Photon Interactions: Basic Processes and Applications* (Wiley, New York, 1992).
[22] D. N. Zubarev, V. Morozov, and G. Röpke, *Statistical Mechanics of Nonequilibrium Processes* (Akademie Verlag, Berlin, 1996).
[23] E. W. Smith, J. Cooper, and C. R. Vidal, Phys. Rev. **185**, 140 (1969).